

Discovery of an operon that participates in agmatine metabolism and regulates biofilm formation in *Pseudomonas aeruginosa*

Bryan J. Williams,^{1*} Rui-Hong Du,² M. Wade Calcutt,³ Rasul Abdolrasulnia,² Brian W. Christman² and Timothy S. Blackwell²

¹Pulmonary, Allergy, Critical Care and Sleep Medicine, University of Minnesota, 420 Delaware St. SE MMC 276, Minneapolis, MN 55455, USA.

²Division of Allergy, Pulmonary, Critical Care Medicine and ³Department of Biochemistry, Vanderbilt University Medical Center, Nashville, TN 37232, USA.

Summary

Agmatine is the decarboxylation product of arginine and a number of bacteria have devoted enzymatic pathways for its metabolism. *Pseudomonas aeruginosa* harbours the *aguBA* operon that metabolizes agmatine to putrescine, which can be subsequently converted into other polyamines or shunted into the TCA cycle for energy production. We discovered an alternate agmatine operon in the *P. aeruginosa* strain PA14 named *agu2ABCA'* that contains two genes for agmatine deiminases (*agu2A* and *agu2A'*). This operon was found to be present in 25% of clinical *P. aeruginosa* isolates. *Agu2A'* contains a twin-arginine translocation signal at its N-terminus and site-directed mutagenesis and cell fractionation experiments confirmed this protein is secreted to the periplasm. Analysis of the *agu2ABCA'* promoter demonstrates that agmatine induces expression of the operon during the stationary phase of growth and during biofilm growth and *agu2ABCA'* provides only weak complementation of *aguBA*, which is induced during log phase. Biofilm assays of mutants of all three agmatine deiminase genes in PA14 revealed that deletion of *agu2ABCA'*, specifically its secreted product *Agu2A'*, reduces biofilm production of PA14 following addition of exogenous agmatine. Together, these findings reveal a novel role for the *agu2ABCA'* operon in the biofilm development of *P. aeruginosa*.

Introduction

Pseudomonas aeruginosa is a relatively infrequent cause of infection in healthy adults; however, it causes considerable morbidity in immunocompromised patients and is a leading cause of hospital-acquired infections (Richards *et al.*, 1999). The majority of adult patients with cystic fibrosis (CF) have chronic lung infections dominated by *P. aeruginosa* which is widely believed to be the source of most of the mortality in this disease (Davies, 2002). *P. aeruginosa* is an environmental organism capable of infecting a wide range of life forms and has one of the most diversified metabolic arsenals of any described bacterium (Stover *et al.*, 2000). Polyamines are a family of small cationic molecules which play important roles in cell cycle regulation in eukaryotes, and in prokaryotes they are implicated in oxidative stress responses, biofilm development and antibiotic resistance (Demady *et al.*, 2001; Maeda *et al.*, 2006; Patel *et al.*, 2006; Battaglia *et al.*, 2007; Kwon and Lu, 2007). One important precursor to polyamine formation, agmatine, is the product of the arginine decarboxylase pathway and is found throughout nature (Majumder *et al.*, 1992; Raasch *et al.*, 1995; Yanagisawa, 2001; Minic and Herve, 2003; Baumann *et al.*, 2007). While agmatine can be a polyamine precursor in most life forms, diverse secondary roles have evolved. In humans, agmatine can function as a neurotransmitter with specificity to the α 2-adrenoreceptor, and is also capable of nitric oxide regulation (Li *et al.*, 1994; Regunathan and Piletz, 2003).

Pseudomonas aeruginosa contains a number of well-described enzymes in the polyamine synthesis pathway including arginine decarboxylase, agmatine deiminase (AgDI), carbamoylputrescine amidohydrolase and ornithine decarboxylase (Fig. 1) (Mercenier *et al.*, 1980; Nakada *et al.*, 2001; Lu *et al.*, 2002). AgDI activity is pivotal in *P. aeruginosa* polyamine synthesis from arginine because it does not contain the *speB* product agmatinase that converts agmatine directly into putrescine as in other bacteria (Salas *et al.*, 2002). AgDI is currently the only known enzyme that can metabolize agmatine in *P. aeruginosa*. The genetic organization of a *P. aeruginosa* AgDI (*aguBA*) operon has been described and contains a number of conserved features found in agmatine operons

Accepted 30 January, 2010. *For correspondence. E-mail bjwillia@umn.edu; Tel. (+612) 624 0999; Fax (+612) 625 2174.

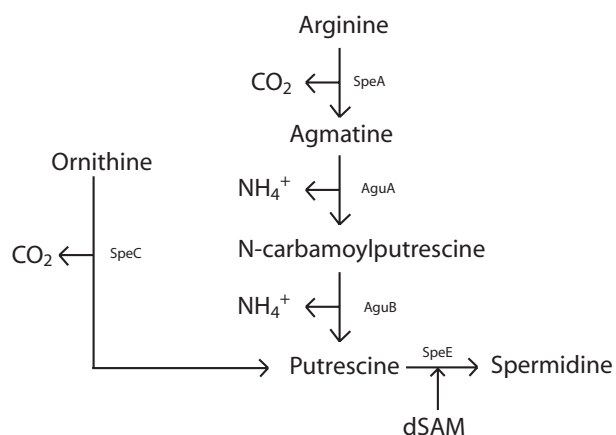


Fig. 1. Polyamine synthesis in *P. aeruginosa*. All enzymes have been experimentally determined to function in *P. aeruginosa* except SpeE for which there is a putative orf in the genome of PAO1. SpeE presence is also implied by the presence of spermidine in *P. aeruginosa* cells. dSAM, decarboxylated S-adenosylmethionine.

of other divergent bacteria (Nakada *et al.*, 2001). Most operons with AgDI (encoded by *aguA*) appear to contain a corresponding *N*-carbamoylputrescine amidohydrolase (*aguB*) and some form of an agmatine inducible or derepressible promoter.

Yersinia pestis has been shown to use polyamines to augment its biofilm formation and the enzymatic pathways for polyamine metabolism are similar to those of *P. aeruginosa* (Patel *et al.*, 2006). Both species contain the *speA* and *speC* genes for arginine and ornithine decarboxylase, respectively, and neither contains an agmatinase gene, suggesting they rely solely on AgDI for agmatine metabolism. While *speA/speC* double mutants of *Y. pestis* show a marked reduction in biofilm development, they appear to have near normal growth in a defined, polyamine-free media. *P. aeruginosa speA/speC* double mutants do not grow unless supplemented with putrescine (Nakada and Itoh, 2003). The role of polyamines in the development of the *P. aeruginosa* biofilm is unknown.

Agmatine deiminase belongs to a superfamily of enzymes called the guanidino-group modifying enzymes (GME) which include a wide range of enzymes spanning prokaryotes to higher eukaryotes, including plants and mammals (Shirai *et al.*, 2006). These enzymes all catalyse the modification of a guanidino group and appear to have strikingly similar functional elements despite very divergent amino acid sequences. Crystallography studies of these enzymes suggest a highly conserved C-terminal cysteine active site is likely critical to their activity (Lu *et al.*, 2006). The genome of *P. aeruginosa* strain PAO1 contains three previously identified examples of the GME superfamily – AgDI (PA0292), arginine deiminase (ADI, PA5171) and dimethylarginase (PA1195) (Tricot *et al.*, 1990). This work describes another group of GME genes

labelled 'porphyromonas peptidyl-arginine deiminase' (PPAD) found in the genome sequence of the pathogenic *P. aeruginosa* strain PA14 but not PAO1 (Shirai *et al.*, 2001). We demonstrate that these genes are part of a putative alternative AgDI operon, henceforth named *agu2ABCA'*, and do not have PADI enzyme activity as their GenBank naming suggests. This work confirms the speculation of a prior comparative analysis that suggests most of the PPAD-designated genes of bacteria are likely AgDI (Shirai *et al.*, 2006). Furthermore we demonstrate that one of the AgDI enzymes is secreted at least to the periplasm, which has not been demonstrated in any previously described bacterial enzyme in the GME superfamily. Promoter expression analyses demonstrate that *agu2ABCA'* is induced by agmatine, but preferentially in the stationary phase and during biofilm growth. We speculated this may have evolved to provide polyamines for biofilm development. Mutant analysis of PA14 revealed a dynamic role for agmatine metabolism in the development of the PA14 biofilm. The inclusion of *agu2ABCA'* into the *Pseudomonas* arsenal of arginine and polyamine metabolism and its function in biofilm development highlight the importance of these enzymatic pathways to the survival of *P. aeruginosa* in the diverse niches it occupies.

Results

Identification of the *agu2ABCA'* operon

The sequence of the putative *agu2ABCA'* operon can be found on GenBank and the PA14 genome project at <http://ausubellab.mgh.harvard.edu/cgi-bin/pa14/home.cgi> (Liberati *et al.*, 2006). The operon spans the PA14 chromosome from base pair 4306779–4311980 as annotated in GenBank. The proposed open reading frames are shown in Fig. 2A. The designation of the first and last ORF in the forward transcript is based on the PFAM motif of 'putative peptidyl arginine deiminase' and corresponds to gene designations PA14 48490 (henceforth named *agu2A*) and PA14 48450 (*agu2A'*). *Agu2A'* contains a genetic sequence to encode for a twin-arginine translocation (tat) signal sequence at its 5' end as predicted by the online program TatP 1.0 located at <http://www.cbs.dtu.dk/services/TatP/> (Bendtsen *et al.*, 2005). The ORFs between *agu2A* and *agu2A'* code for a putative *N*-carbamoylputrescine amidohydrolase (PA14 48470/*agu2B*) and a probable polyamine binding/transport protein (PA14 48450/*agu2C*). There is a 'lysR' transcriptional regulator (PA14 48500/*agu2R*) coded on the opposite reading strand of these four genes. Two potential promoters with their transcription start sites (TSS) are identified in the intergenic region between *agu2R* and *agu2A* (Fig. 2B) by the online neural network promoter prediction available at http://www.fruitfly.org/seq_tools/

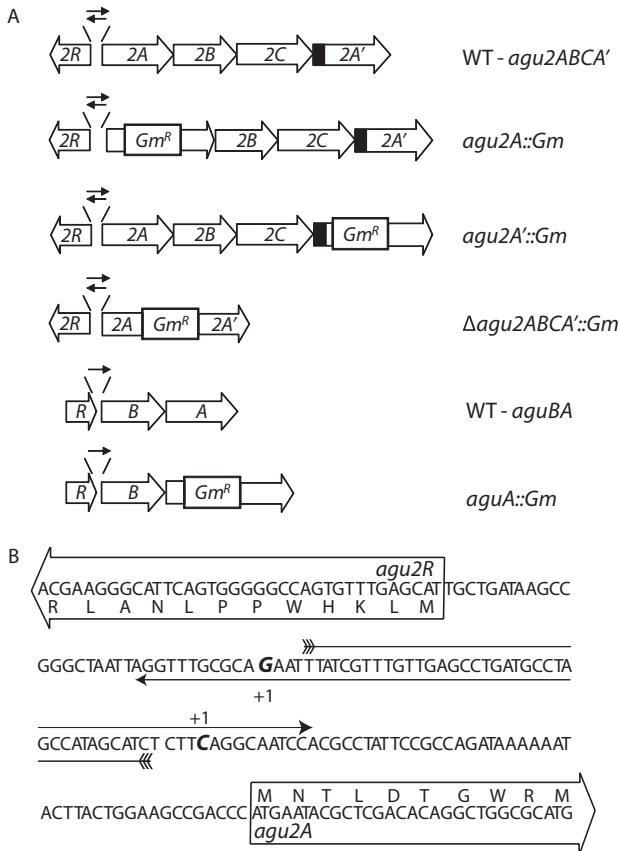


Fig. 2. The *agu2ABCA'* and *aguBA* operons of PA14 and select mutants.

A. The *agu2ABCA'* operon contains two agmatine deiminase genes *agu2A* and *agu2A'*. The black box in gene *agu2A'* designates a tat secretion peptide. The promoter region for this operon is denoted with arrows between *agu2R* and *agu2A* and is shown in B. The *aguBA* operon has been described (Nakada *et al.*, 2001) and is shown for comparison. Open reading frames shown in approximate scale to relative base pair length. The *agu2ABCA':Tet* construct (not shown) is the same as the *agu2ABCA':Gm* except a TetR cassette replaces the GmR cassette.

B. The intergenic region between *agu2R* and *agu2A* contains two putative promoters designated by thin arrows. The transcription starts sites (TSS) are designated as +1 and the TSS for *agu2A* has been experimentally verified.

promoter.html (Reese, 2001). The transcription start site for the mRNA containing *agu2A* and beyond was experimentally determined and found to agree with the predicted TSS. The DNA flanking this operon is nearly identical to a long stretch of PAO1 genome and the entire operon appears inserted into a probable NADPH dehydrogenase gene designated PAO11225. The PAO1 genome base pairs show homology to position 1327795 before the operon and position 1327861 after the operon which is a loss of 66 base pairs in the acquisition of this operon into a conserved 'backbone'. The *agu2ABCA'* operon is not prevalent in many other sequenced organisms and its best match is found in a sequence from *Pseudomonas ento-*

mophila strain L48 showing 78% nucleotide identity over the entire operon.

The prevalence of the *agu2ABCA'* operon in *P. aeruginosa* was determined in a panel of 64 clinical isolates, 16 of which were from the airways of patients with CF. We performed colony PCR screening of all of these strains as well as the laboratory strain PA103 for *aguA*, *agu2A* and *agu2A'*. While every *P. aeruginosa* tested was positive for *aguA*, 25% were positive for both *agu2A* and *agu2A'* as was PA103 suggesting the entire operon is conserved in these strains. While the clinical details of all 64 isolates are not known, the isolates harbouring *agu2ABCA'* operon represent a wide range of infections including those of the urine, sputum, tracheostomy site and a skin ulcer. Only one of the 16 CF isolates was positive for the *agu2ABCA'* operon, and this strain was mucoidy.

Enzymatic properties of *Agu2A* and *Agu2A'*

While the GenBank nomenclature suggested the purpose of this operon may involve PPAD activity, its genetic arrangement suggested it is likely involved in agmatine metabolism. To investigate substrate specificity, both *agu2A* and *agu2A'* were cloned into expression vectors bestowing a C-terminal 6-His tag for identification and purification. The purification of *Agu2A*, *Agu2A'* and an active site mutant of *Agu2A'* is shown in Fig. 3A and the resulting enzymatic activities in Table 1. *Agu2A* with the C-terminal 6-His tag is predicted to be 40.1 kDa while *Agu2A'* with the C-terminal 6-His tag is predicted to be 43.4 kDa with its tat signal peptide intact, or 39.9 kDa when cleaved. Given that the purified protein bands of *Agu2A* and *Agu2A'* are very similar, it is likely that most of *Agu2A'* is present in its cleaved form. Both of these purified enzymes were tested against the appropriate substrates for arginine deiminase activity (ADI) (data not shown), peptidylarginine deiminase activity (PADI) (data not shown) and AgDI activity. Only agmatine served as a substrate in this assay for guanidino conversion to carbamido.

The K_m and K_{cat} values of *Agu2A* and *Agu2A'* are shown in Table 1. The K_m and K_{cat} of *AguA* has been previously shown to be 0.6 ± 0.05 mM and 4.2 ± 0.2 s⁻¹ respectively (Nakada and Itoh, 2003). These calculations were performed at 37°C for *Agu2A* and 25°C for *Agu2A'* to overcome enzymatic instability during initial velocity determinations. *Agu2A* appears closely related to *AguA* in affinity for agmatine and given its proximity to *agu2B* and lack of secretory signal it would appear these cytosolic enzymes are more closely related than either is to the unique *Agu2A'*. A protein BLAST search at NCBI reveals the protein sequences of *Agu2A* and *Agu2A'* only share 41% and 33% identity, respectively, to *AguA* and only 36% identity between each other. Despite the lack of amino

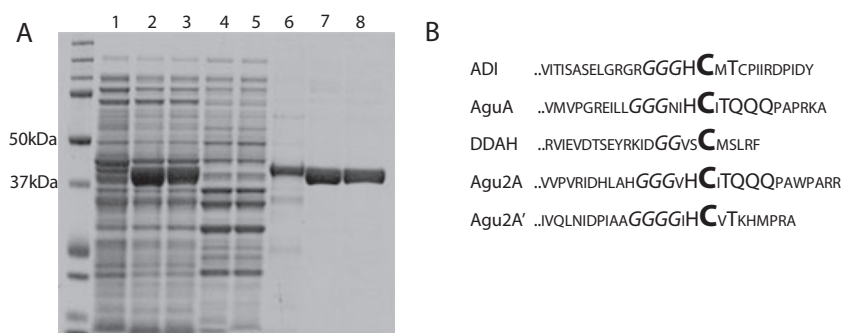


Fig. 3. Agu2A and Agu2A' are agmatine deiminase enzymes with a conserved C-terminal cysteine active site.

A. Coomassie stained gel with crude cell lysates (1–5) or nickel column purified fractions (6–8) of arabinose induced TOP10 cultures harbouring plasmids expressing the following proteins: 1. Agu2A, 2. Agu2A', 3. Agu2A':C364G, 4. Agu2A' with no arabinose induction, 5. TOP10 cloning strain, 6. Agu2A eluate, 7. Agu2A' eluate, 8. Agu2A' C364G eluate. See Table 1 for corresponding enzymatic activities.

B. Comparison of the C-terminal amino acid sequences of members of the guanidino modifying enzymes found in *P. aeruginosa*. Conserved amino acids are highlighted and have been described (Shirai *et al.*, 2006).

acid homology the functional relationship between AguA and Agu2A is also supported by the conserved poly-glutamine region just after the cysteine active site (Fig. 3B) which is absent in Agu2A'.

The predicted protein sequences of Agu2A and Agu2A' both share C-terminal residues important for enzymatic activity in other GME superfamily members (Fig. 3B). To define the active site in Agu2A', and to serve as a purification control, we mutated the plasmid pBW421 harbouring *agu2A'* to express glycine instead of cysteine at residue 364, the putative active site of this enzyme. The protein from this mutant was expressed and purified in an identical fashion to its non-mutated parent (Fig. 3A), but has no AgDI activity in either the crude cell lysate or in the purified mutant protein (Table 1).

The comparative, enzymatic and mutational analyses all supported the hypothesis that the AguA orthologues of the *agu2ABCA'* operon both functioned as AgDI enzymes, not PADI enzymes, and Agu2A' absolutely requires the C-terminal cysteine at position 364 for its activity.

Secretion of Agu2A'

The proposed protein sequence of Agu2A' contains a twin-arginine translocation (tat) sequence at its

N-terminus shown in Fig. 4A. The twin-arginine motif is so named as the arginines appear to be required for appropriate secretion by the tat system (Lee *et al.*, 2006). To determine if this signal sequence directs secretion of Agu2A', the twin arginine motif was mutated to glycine-serine in plasmid pBW42101 harbouring an inducible, 6-His-tagged Agu2A' in an *E. coli*/*P. aeruginosa* shuttle vector. The resultant plasmid, pBW42151, and its parent plasmid were transformed into PAO1 and induced with 0.2% arabinose in Luria–Bertani (LB). The cells were fractionated into spheroplasts, which contain the inner membrane and cytosol, periplasm/outer membrane and culture supernatant. Protein precipitates of these fractions were analysed by Western blot using the anti-C-terminal 6-His antibody as demonstrated in Fig. 4B. NADH oxidase was measured as a cytoplasmic control enzyme and β -lactamase as a periplasmic protein as previously described (Snyder *et al.*, 2006). The samples used in Fig. 4B show > 90% of the total NADH oxidase activity was retained in the spheroplast fraction and > 99% of the β -lactamase activity was present in the periplasmic and spent media fractions of both strains (data not shown). The wild type Agu2A' is much more abundant in the periplasmic fraction than its twin-arginine mutant demonstrating that Agu2A' is secreted through the inner membrane

Table 1. Specific activities and enzymatic rates of AgDI enzymes.

Induced protein / sample	Specific activity ^a	Km/Kcat ^b
Agu2A/crude cell lysate	0.0298 ± 0.0003	ND
Agu2A'/crude cell lysate	0.135 ± 0.001	ND
Agu2A' C364G/crude cell lysate	< 0.0001	ND
Agu2A/column eluate	0.901 ± 0.061	0.136 ± 0.040 / 14.12 ± 0.49
Agu2A'/column eluate	0.633 ± 0.030	2.624 ± 1.125 / 33.27 ± 4.22
Agu2A' C364G/column eluate	< 0.0001	ND

a. Specific activity is in nmol citrulline equivalents h⁻¹ μg⁻¹ protein ± SEM.

b. Km is expressed in mM ± SEM and Kcat is s⁻¹ ± SEM.

ND – not determined.

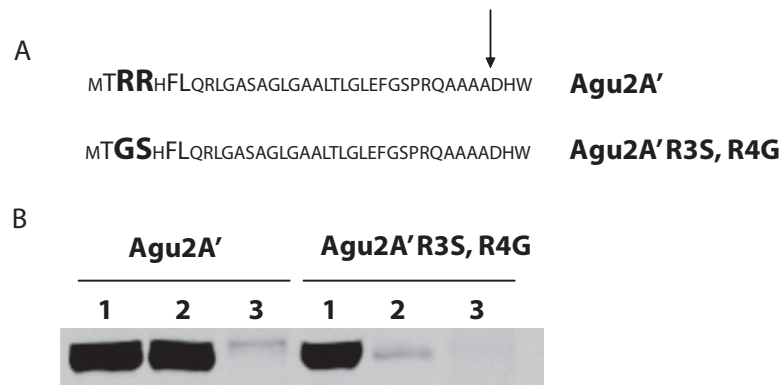


Fig. 4. Agu2A' is secreted into the periplasm through the twin-arginine translocase system.

A. N-terminal amino acid sequence of Agu2A' and its secretion mutant demonstrating the predicted twin arginine consensus sequence (critical amino acids are highlighted) and the proposed cleavage site in the wild type strain (arrow).

B. Western blot to C-terminal 6-His tag of protein fractions from Agu2A' or Agu2A' R3S, R4G expression vectors induced with arabinose in strain PAO1. Cell fractionation is designated as 1. Inner membrane, cytosol, 2. Outer membrane, periplasm, 3. Supernatant. Each lane was loaded with 15 µg of protein from the various fractions. See *Results* section for description of the enzymatic assays used to ensure proper fractionation.

by the twin-arginine translocase system. A faint band is also seen in the supernatant fraction suggesting it may also traverse the outer membrane in limited quantities. While the predicted secretion product of Agu2A' is 39.9 kDa compared with 43.4 kDa for the unsecreted form, a distinct size difference was not seen between the cytoplasmic and periplasmic fractions. While this may simply have been an inability to resolve a 3.5 kDa difference in our electrophoresis system, it also suggests cleavage occurs in the inner membrane in both wild-type and mutant or that another post-translational modification occurs in the periplasm that changes its electrophoretic mobility. The presence of a faint band in lane 2 of the mutant is likely explained by the slight cytoplasmic spillage detected with the control NADH oxidase analysis rather than true secretion. The secretion of Agu2A' into the periplasm via the *tat* system is a unique feature of this operon and suggested the purpose of *agu2ABCA'* is not a duplication of the metabolic role of *aguBA*.

Agu2ABCA' complementation of AguBA

PAO1 and PA14 can use agmatine as their sole carbon and nitrogen source in liquid or solid media growth. The *aguBA* operon was shown to be critical for this growth in PAO1 with *aguA* absolutely required (Nakada *et al.*, 2001). We sought to determine if the *agu2ABCA'* operon could play a role in agmatine metabolism in a manner that could restore the growth of an *aguA* mutant grown in agmatine minimal media. We were generously given *aguA* transposon mutants of both PAO1 and PA14 as well as *agu2A*, and *agu2A'* in PA14. We also introduced the entire *agu2ABCA'* operon in an *E. coli*/*P. aeruginosa* shuttle vector into the PAO1 *aguA* mutant, which normally

does not contain the *agu2ABCA'* operon. We also generated *agu2ABCA'* operon deletions in both PA14 and the *aguA* mutant of PA14 using a suicide vector as described in the *Experimental procedures* section. Table 2 shows the growth of these mutants on minimal media supplemented with agmatine with or without other carbon or nitrogen sources. This experiment demonstrated that *aguA* makes agmatine available as a carbon and nitrogen source in PAO1 and PA14. In the absence of *aguA*, *agu2ABCA'* was capable of complementation when present on a multicopy plasmid as in the PAO1 *aguA* mutant, or in its genomic configuration as in the PA14 *aguA* mutant. When gluconate was supplied as a carbon source, *agu2ABCA'* appeared to readily metabolize agmatine to provide a nitrogen source allowing growth. This is likely given that *agu2A*, *agu2B* and *agu2A'* all liberate ammonia during their proposed enzymatic step. When no supplemental carbon source was provided, *agu2ABCA'* weakly converted agmatine into a sufficient carbon source to allow for growth of very small colonies after 3 days. Loss of either *agu2A* or *agu2A'* alone or together did not result in a phenotype different from wild-type PA14. When both *aguA* and *agu2ABCA'* are removed from PA14, no growth was observed on any of the agmatine minimal media plates. When agmatine was not provided in this system, no growth occurred in any strains after 4 days and all strains grew at the same rate when grown in a rich media (data not shown). The presence of *agu2ABCA'* on a multicopy shuttle vector allowed for a slightly faster utilization of agmatine as a carbon source than when present in a single copy on the chromosome. Re-streaking any of these colonies after growth on agmatine minimal media did not change the rate of growth on fresh agmatine minimal media plates,

Table 2. Complementation phenotype of AgDI mutants.

Strain	AgDI genes present	Growth ^a on MM + Agm ^b	Growth on MM + NH ₄ + Agm	Growth on MM + gluconate + Agm
PAO1	<i>aguA</i>	+++ , 1 d	+++ , 1 d	+++ , 1 d
PAO5001	–	–	–	–
PAO5001 + pBW110	<i>agu2A, agu2A'</i> ^c	+, 3 d	+, 3 d	++, 2 d
PA14	<i>aguA, agu2A, agu2A'</i>	+++ , 1 d	+++ , 1 d	+++ , 1 d
PA14.27633	<i>aguA, agu2A'</i>	+++ , 1 d	+++ , 1 d	+++ , 1 d
PA14.48017	<i>aguA, agu2A</i>	+++ , 1 d	+++ , 1 d	+++ , 1 d
PA14.521	<i>aguA</i>	+++ , 1 d	+++ , 1 d	+++ , 1 d
PA14.42664	<i>agu2A, agu2A'</i>	+/- , 4 d	+/- , 4 d	++, 2 d
PA14.42664.521	–	–	–	–

a. Growth phenotype quantified after number of days indicated. +++ clearly visible growth with distinct colonies, ++ clearly visible growth with smaller colonies, + growth visible over areas of heavier streaking, no distinct colonies, +/- microcolonies visible over areas of heavy streaking when viewed under magnification, – no growth seen in any portion under magnification.

b. See *Experimental procedures* for description of minimal media composition.

c. AgDI genes located within multicopy plasmid.

which shows these were not *aguA* mutant revertants (data not shown). These data suggest *agu2ABCA'* is active and capable of metabolizing agmatine, however, at a different rate or possibly phase of growth than *aguBA*.

Regulation of *agu2ABCA'* expression

While the enzymatic analysis suggests the AgDI function of *agu2ABCA'* is not grossly different than *aguA*, its lack of robust complementation of *aguA* mutants suggests its regulation may be different, supporting the notion that *agu2ABCA'* may have evolved for a different role in agmatine metabolism. To better understand the regulation of *agu2ABCA'*, we cloned the putative promoter region between *agu2R* and *agu2A* into the mini-ctx-lacZ reporter vector and analysed its expression after integration into the PA14 and PAO1 chromosomes at the innocuous *attB* site (Becher and Schweizer, 2000). As shown in Fig. 5A and Fig. S1A we cloned the *agu2ABCA'* promoter region with and without the orf for *agu2R*, a putative 'lysR' regulator. We also cloned the *aguBA* promoter with *aguR*, which encodes a tetR transcriptional regulator that was previously shown to constitutively bind the *aguBA* promoter until derepressed by agmatine (Nakada *et al.*, 2001). While a similar growth curve was observed for bacteria containing *aguBA* and *agu2ABCA'* promoter-reporter constructs (Fig. 5B) a differential expression pattern for these intact promoters was identified following the addition of agmatine (Fig. 5C). While *aguBA* was induced early during log phase, *agu2ABCA'* had a delayed expression until the start of stationary phase. We hypothesized that this delay could be the result of agmatine depletion by *AguA* which is expressed earlier, so we also tested the *agu2ABCA'* promoter-reporter in a *aguA::Gm* mutant of PA14. Mutation of *aguA* does increase the magnitude of *agu2ABCA'* expression in expression but does not cause it to be expressed earlier. The delayed

agmatine-induced expression of *agu2ABCA'* was further examined by allowing the reporter strains to grow to stationary phase before exposure to agmatine. Figure 5D demonstrates a much faster expression of the *agu2ABCA'* promoter when stimulated with agmatine after reaching stationary phase. In contrast, stimulation of reporter strains with glutamine at stationary phase resulted in little differences versus unstimulated cultures (Fig. 5E) which suggests the response to agmatine is specific and not simply one of nutrient repletion. We also tested the *agu2ABCA'* promoter-reporter in PA14-based mutants of *rpoS* and *lasR* which are both well-known regulators of stationary phase genes in *P. aeruginosa* (Schuster *et al.*, 2004; D'Argenio *et al.*, 2007). Compared with WT PA14 we observed no differences in the β -gal response between any of these strains, suggesting neither *rpoS* nor *lasR* regulate *agu2ABCA'* (data not shown).

To better understand the nature of the putative 'lysR' regulator *Agu2R*, we generated a reporter construct that did not include the entire coding sequence of *Agu2R* but preserved the putative promoter region between *agu2R* and *agu2A* as shown in Fig. S1A and tested the constructs in PAO1 which does not harbour a copy of *agu2ABCA'*. With the laboratory domestication of PAO1, it is believed to have acquired mutations in its genetic regulatory networks as it displays different phenotypes between various laboratories (Friedman and Kolter, 2004; Tremblay and Deziel, 2008). Thus we repeated the growth curves and expression assays in PAO1 performed in Fig. 5 assuming they would show a different baseline than PA14. Fig. S1C–F shows that the *agu2ABCA'* promoter requires both the *agu2R* orf and agmatine to be activated, and maximal expression occurs in stationary phase. This experiment also shows that the *agu2ABCA'* promoter has much more activity in PAO1, especially in stationary phase where its activity is almost 10-fold higher than the *aguBA* promoter.

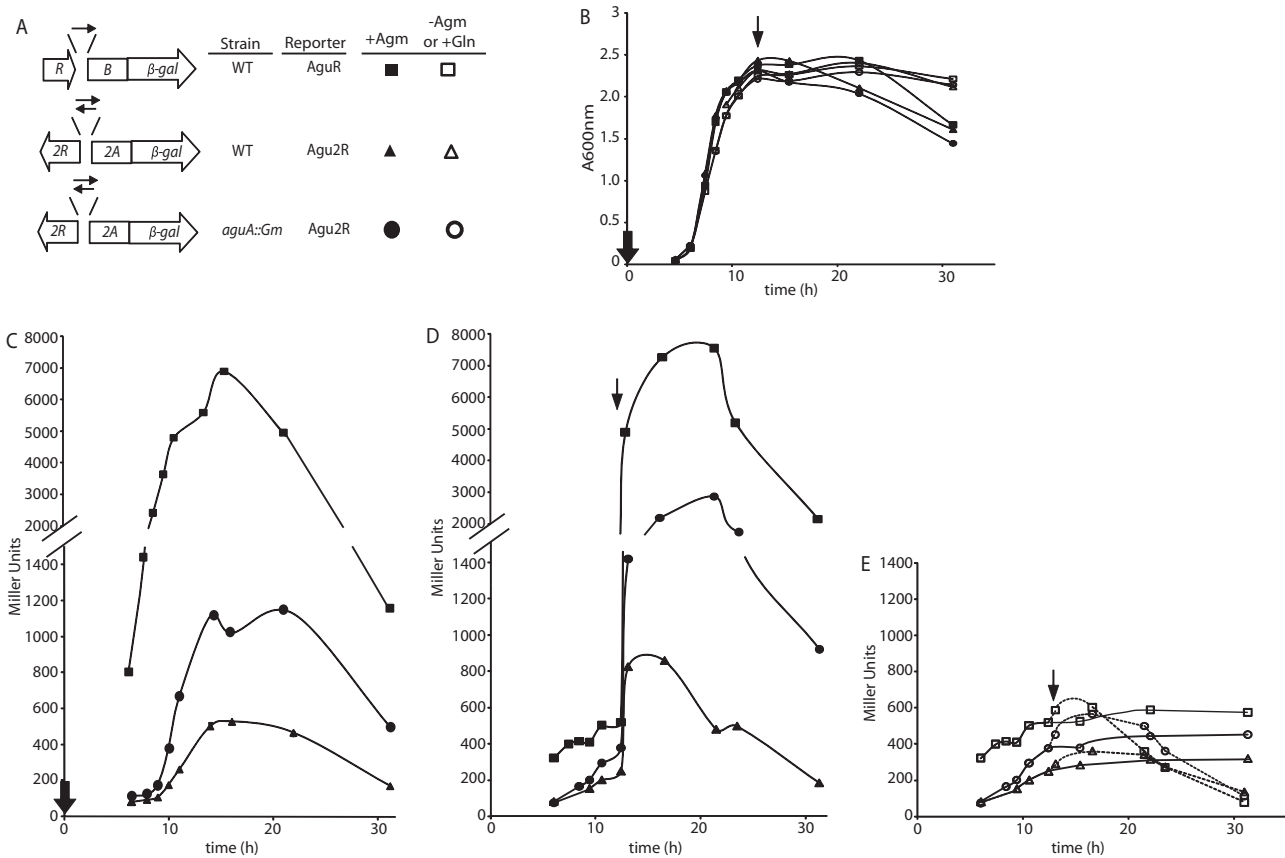


Fig. 5. Expression profile of agmatine operons during planktonic growth.

PA14 or its *aguA::Gm* mutant harbouring the reporter constructs shown in (A) were grown in liquid culture with or without supplements and samples were measured for β -gal activity at various times during the growth curve. For B–E \downarrow indicates agmatine addition at inoculation and \downarrow indicates agmatine or glutamine addition at entry to stationary phase (agmatine or glutamine added to 20 mM final concentration; LB media used in all experiments). Dashed lines represent growth with glutamine. B. Growth curve of the reporters used in studies shown in parts C–E. C. β -gal expression with agmatine supplementation at inoculation. D. β -gal expression with agmatine supplementation at stationary phase. E. β -gal expression with and without glutamine supplementation at stationary phase. ‘Empty’ reporter constructs express < 200 Miller units regardless of supplement or growth condition (data not shown). β -gal assays performed at each timepoint from same culture in triplicate and SEM < 1% for most points (data not shown).

AgDI influence on intracellular agmatine

As the AgDI enzymes of *P. aeruginosa* are expressed during different phases of growth and appear to function in different cellular locations, we sought to determine if the agmatine concentration within the cell was influenced by AgDI activity. The complementation data suggest *aguBA* is the dominant AgDI operon within the cell. To determine if *agu2ABCA'* could influence the intracellular agmatine pools, we used mass spectrometry to measure the intracellular agmatine of cultures that were grown specifically to induce *agu2ABCA'*. After 18 h of growth in LB, PA14 and select AgDI mutants were stimulated with either agmatine or glutamine and allowed to grow for 3 more hours. Table 3 shows the agmatine concentration within the lysed cell pellets. These data demonstrate that PA14 with intact AgDI enzymes metabolizes intracellular

Table 3. Intracellular agmatine concentration in AgDI mutants.

Strain/mutant and supplement ^a	Intracellular agmatine ^b \pm SEM
PA14 + Gln	< 0.001 ^c
PA14 + Agm	< 0.001 ^c
PA14 <i>aguA::Gm</i> + Gln	0.922 \pm 0.076
PA14 <i>aguA::Gm</i> + Agm	12.41 \pm 0.22
PA14 <i>agu2A'::Gm</i> + Gln	0.0321 \pm 0.0026
PA14 <i>agu2A'::Gm</i> + Agm	0.0300 \pm 0.0185

a. Glutamine or agmatine was added to a final concentration of 20 mM after cultures grown in supplement free LB for 18 h. Cell pellets were collected for agmatine extraction after 3 h growth in supplement.

b. Value shown is average of three samples from same culture processed independently and expressed as $\mu\text{mol agmatine g}^{-1}$ wet cell pellet. This experiment was repeated once with similar results.

c. Value below assay detection limit.

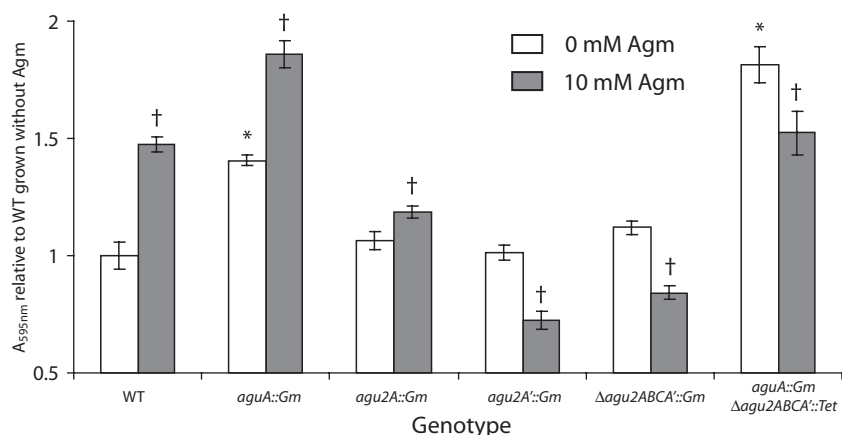


Fig. 6. Agmatine metabolism regulates the PA14 biofilm. PA14 and its AgDI mutants were grown overnight in LB media in 96-well polystyrene plates with or without supplemental agmatine (10 mM shown here). Crystal violet staining of the biofilm and quantification at A_{595nm} was performed as described in the *Experimental procedures*. Each data point represents the average of eight wells and error bars are \pm SEM. Comparison groups were all grown on the same plate and strains grown at 10 mM Agm were compared with the same strain grown at 0 mM Agm for statistical analysis (see Fig. S2 for Agm dose–response of each mutant). These results were confirmed with > 3 repeat assays. **P* < 0.0001 compared with WT grown without Agm. †*P* < 0.0001 compared with same strain grown without Agm.

agmatine to levels below the sensitivity of our assay; however, removal of *aguA* or *agu2A'* results in agmatine accumulation. The presence of intracellular agmatine in the *agu2A'* mutant suggests a small portion of agmatine is not effectively eliminated by AguA, but is accessible to Agu2A' most likely within the periplasm.

The high agmatine concentrations within the *aguA* mutant grown without agmatine suggests high activity of arginine decarboxylase to generate agmatine, or efficient acquisition from LB media which contains approximately 3 μ M agmatine (determined in data not shown). Addition of agmatine to the media of the *aguA* mutant results in a large increase in intracellular agmatine. This latter finding is not seen with the *agu2A'* mutant where the unmetabolized agmatine pool is essentially unchanged. This suggests the periplasmic agmatine supply is relatively stable compared with the cytosol.

Agu2ABCA' enhances biofilm development in PA14

The clear delineation between the expression profiles of *aguBA* and *agu2ABCA'* suggested a separate biological purpose for *agu2ABCA'* such as providing polyamines or free ammonia to non-rapidly dividing Pseudomonads, or those in high cell densities or biofilms. To determine if AgDI genes contribute to biofilm formation in *Pseudomonas*, we tested PA14 AgDI mutants in a well-described 96-well microtiter plate biofilm assay with crystal violet staining of adherent bacteria (O'Toole and Kolter, 1998). When grown in rich media without supplemental agmatine, deletion of *aguA* augmented biofilm development, and the biofilm was further increased by combined deletion of *aguA* and *agu2ABCA'* (Fig. 6). In addition, WT

PA14 grown in the presence of increasing agmatine concentrations show a dose-dependent increase in biofilm development (Fig. 6 and Fig. S2). Together, these data suggested that agmatine augments the biofilm of PA14 and its metabolism reduces it. However, further analysis of the individual mutants grown in the presence of agmatine revealed a more complicated regulation. When *aguA* alone was deleted, the response to agmatine was similar to WT, but when *agu2A'* or the entire *agu2ABCA'* operon was mutated, agmatine inhibited the biofilm in a dose-dependent manner (Fig. 6 and Fig. S2). This finding indicates that *agu2ABCA'*, specifically the periplasmic AgDI Agu2A', is responsible for the agmatine-induced augmentation of the PA14 biofilm.

We further addressed this finding by testing our promoter-constructs during biofilm growth in PA14 (Fig. 7). We disrupted the bacteria containing reporter constructs remaining on the walls of plastic dishes with sonication and chemical lysis and measured the liberated β -galactosidase compared with the total liberated protein as a surrogate measure to the Miller assay (Sakuragi and Kolter, 2007). This experiment revealed an agmatine-induced expression of both *aguBA* and *agu2ABCA'* during biofilm growth; however, *agu2ABCA'* was preferentially expressed when agmatine was added to already-established biofilms.

The biofilm of PA14 is fairly well described and has been shown to differ in composition from PAO1 (Wozniak *et al.*, 2003; Friedman and Kolter, 2004). We tested PAO1 harbouring a plasmid borne copy of *agu2ABCA'* in these assays but were not able to elucidate any differences in the biofilm phenotype (data not shown). This suggests other PA14 specific genes are necessary for this

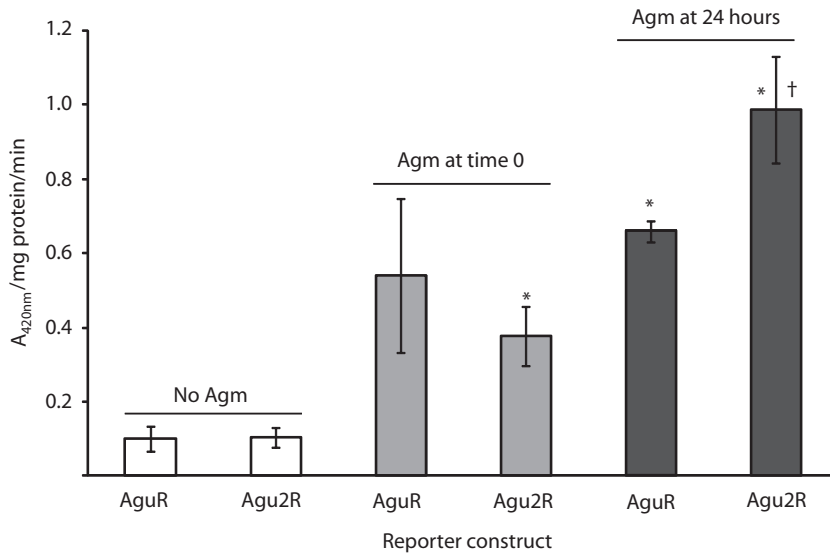


Fig. 7. Expression profile of agmatine operons during biofilm growth. PA14 Biofilms were grown as described in Fig. 6 except 24-well polystyrene plates were used. Reporter configuration shown in Fig. 5. Biofilm growth was harvested as described in *Experimental procedures* at 27 h growth and analysed for β -gal activity. Assays were done in triplicate and error bars are \pm SEM. Agmatine was added to a final concentration of 10 mM either at inoculation (time 0) or after 24 h of growth without agmatine. * $P < 0.05$ compared with the same reporter grown without agmatine. † $P < 0.05$ compared with same reporter grown with agmatine from time 0.

agmatine-induced biofilm phenotype. We also tested the effect of putrescine in this system to determine if polyamine addition would complement some of the mutant phenotypes (Fig. S2B). Unlike agmatine titration, putrescine titration had no effect on biofilm formation in any mutant and became toxic at concentrations above 1 mM.

Our working model of these data is presented in Fig. 8. In summary, these data suggest that cytosolic AgDI metabolism inhibits biofilm development, whereas periplasmic AgDI metabolism enhances biofilm development. As the periplasmic AgDI is specifically induced during biofilm growth, and appears responsible for periplasmic agmatine removal, it is possible that *agu2ABCA'* evolved

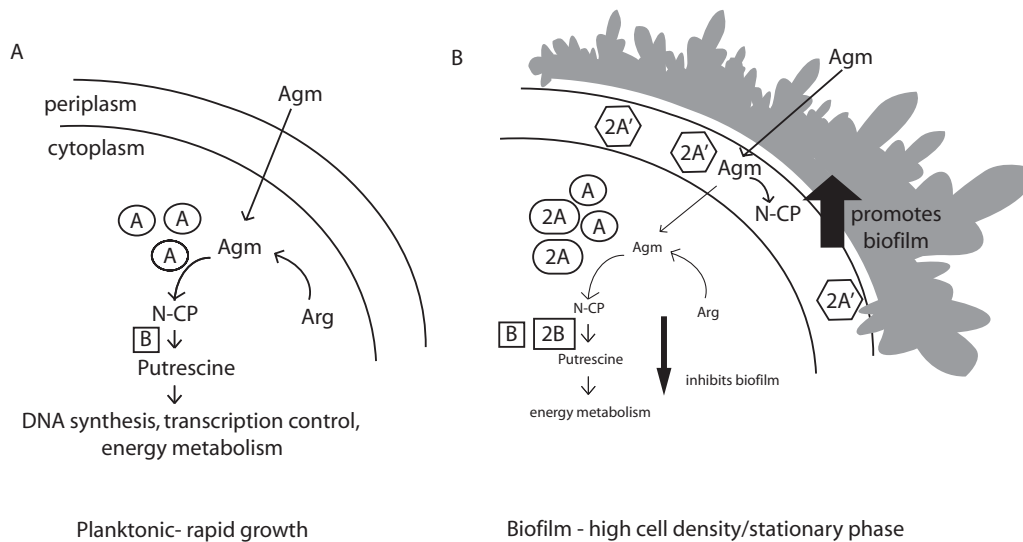


Fig. 8. Agmatine regulation of biofilm development.

A. During rapid growth agmatine (Agm) is created in the cytoplasm by arginine (Arg) decarboxylase or traverses the cell wall if exogenous agmatine is available. *AguBA* is upregulated and agmatine is metabolized to *N*-carbamoylputrescine (*N*-CP) and ultimately putrescine by the successive actions of *AguA* and *AguB*. Putrescine is used for a number of processes involved in cell division and can be used for energy production.

B. During biofilm growth, exogenous agmatine traverses the cell wall and distributes to both the cytosol and periplasm. In the cytosol agmatine preferentially stimulates transcription of *agu2ABCA'* which results in *Agu2A'* production and secretion to the periplasm, as well as production the cytosolic enzymes *Agu2A* and *Agu2B*. Exogenous agmatine stimulates the PA14 biofilm through its periplasmic metabolism, and this effect is dominant to the inhibitory effect of cytosolic agmatine metabolism. As *agu2ABCA'* weakly complements the *aguA* mutant, it can metabolize agmatine for use as a sole carbon and nitrogen source, presumably through the actions of the cytosolic *Agu2A* and *Agu2B*.

to regulate the biofilm response to exogenous agmatine in *P. aeruginosa*.

Discussion

We have discovered a second putative agmatine operon in *P. aeruginosa* and have experimental evidence that two of the genes code for proteins that catalyse the deimination of agmatine to the polyamine precursor *N*-carbamoylputrescine. While polyamines have a myriad of purposes in bacteria, we investigated the *P. aeruginosa* biofilm and determined that *agu2ABCA'* enhances its development. Several characteristics of the *agu2ABCA'* operon suggested it may play a role in biofilm development. First, there is a precedence for polyamines in the biofilm development of *Y. pestis*, which shares similar polyamine enzymatic pathways with *P. aeruginosa* (Patel *et al.*, 2006). Second, the secretion of *Agu2A'* suggests the enzymatic step may be occurring in the periplasm or cell surface where a number of important processes in biofilm development occur (Mah *et al.*, 2003; Campisano *et al.*, 2006). Third, the twin-arginine translocation system responsible for the secretion of *Agu2A'* is upregulated in *P. aeruginosa* grown as a biofilm (Whiteley *et al.*, 2001). Finally, the preferred expression in stationary phase suggested *agu2ABCA'* may be providing polyamines for a maintenance or reparative process over one of energy creation or stabilization of DNA synthesis.

More work is necessary to unravel the contribution of *agu2ABCA'* to the chemical composition of the PA14 biofilm; however, it is possible that the periplasmic conversion of agmatine to *N*-carbamoylputrescine influences the synthesis or secretion of polysaccharides either through alkalization from the deimination of agmatine or through an effect mediated by the accumulation of *N*-carbamoylputrescine. Addition of exogenous putrescine did not appear to have an effect on the biofilm phenotype. This could be expected as putrescine does not inhibit the AgDI enzymatic step (Nakada and Itoh, 2003). As the mechanism of biofilm enhancement may occur in the periplasm, it is not clear if exogenous putrescine addition would result in a periplasmic accumulation. Ideally, measurement of agmatine and *N*-carbamoylputrescine within the periplasm of cells, grown planktonically and as a biofilm, would begin to unravel this mechanism. We attempted to measure periplasmic agmatine for this study however, the fractionation process used for protein localization was not effective on stationary phase bacteria judged by poor partitioning of our control enzymes (see *Experimental procedures*).

Agu2ABCA' is clearly not essential for biofilm development in all *P. aeruginosa* as it is not present in PAO1, a known biofilm former, or more than half of the clinical strains we tested. Furthermore, *agu2ABCA'* appears to

have little to no impact on the PA14 biofilm when grown without exogenous agmatine. These studies show that *agu2ABCA'* was probably adapted from a strictly metabolic role, to one of environmental adaptation likely brought about by a hostile environment containing agmatine. As agmatine does not appear to be directly toxic to *P. aeruginosa*, it would suggest agmatine could be a marker of other stressful conditions. Macrophages secrete agmatine when stimulated with endotoxin (Regunathan and Piletz, 2003). We have measured agmatine concentrations in the sputum of patients with CF and have shown it is positively correlated with markers of inflammation including IL1 β , IL8 and TNF α (unpubl. data). Agmatine may be a direct initiator of inflammation in mammals as both neutrophils and macrophages harbour α 2-adrenoreceptors that have been implicated in endotoxin induced lung inflammation (Flierl *et al.*, 2007). We have also observed that agmatine is capable of inducing TNF α release from macrophages in a α 2-adrenoreceptor-dependent mechanism (unpubl. data). As biofilms are associated with persistent infection (Davies, 2002), we speculate that *Pseudomonads* harbouring *agu2ABCA'* may have a survival advantage during infections characterized by marked inflammation, such as the chronic airways infection of CF.

While the enzymatic properties of *agu2ABCA'* initially suggested a duplication of the previously described *aguBA* operon of *P. aeruginosa*, a number of findings distinguish it. In addition to the genes for AgDI enzymes and *N*-carbamoylputrescine amidohydrolase, *agu2ABCA'* also encodes a probable periplasmic polyamine binding protein. The likely purpose of this protein is to shuttle agmatine or *N*-carbamoylputrescine into the cell and putrescine or other downstream products out, as described for the *Lactococcus brevis* orthologue (Lucas *et al.*, 2007). *Agu2A'* is distinguished by its twin-arginine translocation sequence which allows for its transport to the periplasm in *P. aeruginosa*. The *tat* system is highly utilized by *Pseudomonas* species and most of the proteins it secretes are predicted to be involved in redox reactions; however, the *tat* system also appears important for bacterial virulence (Ochsner *et al.*, 2002; Lee *et al.*, 2006). Both *Agu2A* and *Agu2A'* contain the highly conserved C-terminal cysteine active site motif found in all of the GME superfamily members. While crystal structures have been determined for other AgDI that contain this motif, our work shows that mutation of this site completely removes enzymatic function, reinforcing the excellent descriptive work done in this field to date (Tricot *et al.*, 1990). Another important piece of evidence to suggest the lack of functional duplicity between the agmatine operons is their differing regulation. While both are clearly responsive to agmatine, *agu2ABCA'* expression is delayed until early stationary phase whereas *aguBA* expression preferentially occurs during the rapid growth phase. This

divergent regulation explains the slow growth of the *aguA* mutants complemented with *agu2ABCA'*. Their ability to enter stationary phase was reduced in agmatine minimal media as the log phase enzyme for its metabolism was absent. We presumed the genetic regulation of *agu2ABCA'* would be under the control of *rpoS* or *lasR* which have been shown to control a number of genes expressed during the stationary phase or periods of high cell density (Schuster *et al.*, 2004). We did not observe any decreased expression of the *agu2ABCA'* promoter in *rpoS* or *lasR* mutants, thus the regulators of its delayed expression are still unclear. Analysis of *agu2R* expression, and its regulation of the promoter in future studies will help us resolve this remaining question.

Experimental procedures

Bacterial strains, media, growth conditions

Strains and plasmids used in this study are presented in the online Table S1. LB was used as the rich media for *E. coli* and *P. aeruginosa* with antibiotic concentrations for *E. coli*: ampicillin 100 µg ml⁻¹, kanamycin 50 µg ml⁻¹, tetracycline 20 µg ml⁻¹, gentamicin 15 µg ml⁻¹, and for *P. aeruginosa*: carbenicillin 200 µg ml⁻¹, gentamicin 15 µg ml⁻¹, tetracycline 100 µg ml⁻¹. The minimal media for *P. aeruginosa* consists of 10.5 g of K₂HPO₄, 4.5 g of KH₂PO₄ and 48 mg of MgSO₄ per liter of water. For carbon source supplementation sodium gluconate was added to 20 mM, and for nitrogen source supplementation ammonium sulfate was added to 7.5 mM. When indicated agmatine or glutamine was added at 20 mM (Fukuoka *et al.*, 1991). All growth was carried out at 37°C except where indicated.

Plasmid construction and mobilization

Primer description and sequences are presented in the online Table S2. All PCR reactions generated for cloning were performed with the GC-Rich PCR System following manufacturer's recommendations (Roche) in a Veriti Thermocycler (Applied Biosystems). The pCR-XL TOPO TA cloning system (Invitrogen) was used to clone the *agu2ABCA'* PCR product generated from PA14 chromosomal DNA with primers 1F and 1R. This plasmid, pBW100, contains the entire *agu2ABCA'* operon and ~2 kb of flanking chromosomal DNA. To mobilize this operon back into *P. aeruginosa* the EcoRI fragment of this plasmid containing the operon was subcloned into pUCP20 creating pBW110. The *agu2A* and *agu2A'* genes were PCR amplified from PA14 genomic DNA and inserted into pBAD202 TOPO expression system (Invitrogen) per manufacturer's protocol. *Agu2A* was amplified with primers 2F and 2R and *agu2A'* was amplified with primers 3F and 3R. These primers were designed to allow removal of the thioredoxin fusion partner inherent in the pBAD202 system and the 3' stop signal which permits linkage to the 6-His tag in pBAD202 and ultimately the C-terminus of the expressed protein. To create pBW4216, the proposed enzymatic active site (C364) of *Agu2A'* was mutated in pBW421 using the Quick Change

II mutagenesis kit (Stratagene) to change Cys to Gly, creating a *NcoI* site following the manufacturer's protocol with primers 4F and 4R. To move pBW421 into *P. aeruginosa*, the *NsiI*-*PmeI* fragment containing the arabinose promoter, *araC* regulator, and the 6-His-labelled *agu2A'* was cloned into the *PstI*-*SmaI* site of pUCP20 to create pBW42101. To create pBW42151, the twin-arginine translocation sequence of *agu2A'* was mutated in pBW42101 using the Quick Change II mutagenesis kit to change the N-terminus Arg-Arg sequence to Gly-Ser with primers 5F and 5R.

To expand the usefulness of pPS856 we generated a 'tetracycline cassette' version by PCR amplifying the Tet^R cassette from pEX18Tet using primers 6F and 6R which contain *MfeI* sites. The pPS856 'backbone' was amplified using primers 7F and 7R and the EcoRI digest of this product was ligated to the *MfeI* digested product above to generate pPS856Tet. This plasmid retains the flanking multiple cloning sites and FRT sites around the Tet^R cassette.

To make pBW5 we cloned the entire *agu2ABCA'* operon and ~4 kb of flanking chromosomal DNA into the pCR-XL TOPO TA vector using primers 8F and 8R. To generate a suicide vector to delete the entire operon pBW5 was digested with *AgeI* and *NruI*, blunt ended with the NEB 'Quick blunting' enzyme kit, gel purified and ligated to the gentamicin cassette generated from pPS856 treated with *SmaI*. To generate pBW521 the *NheI*-*HindIII* fragment containing the deleted operon and gentamicin cassette was cloned into the *HindIII*-*XbaI* sites in pEX18Ap. To generate pBW521tet, the tetracycline cassette from pPS856tet was removed with *BamHI* and ligated into the *BglIII* site within the gentamicin cassette of pBW521. To make the *agu2ABCA'* chromosomal deletion mutants we moved pBW521 into PA14 and pBW521Tet into the *aguA* mutant of PA14 and isolated sucrose resistant colonies as described elsewhere (Hoang *et al.*, 1998). Loss of *agu2ABCA'* was verified by PCR of chromosomal DNA.

To make pBW71 we cloned the promoter and regulator of the PA14 *aguBA* operon using primers 9F and 9R. The EcoRI/*HindIII* digested product was inserted into the multiple cloning site of the mini-ctx-lacZ reporter plasmid (Becher and Schweizer, 2000). To clone the putative promoter of *agu2ABCA'* we PCR amplified it with (pBW72) and without (pBW73) the *agu2R* orf which codes for the putative transcriptional regulator into the mini-ctx-lacZ reporter plasmid. Primers 10F1 and 10R were used for pBW72 and primers 10F2 and 10R were used for pBW73. The sequences of pBW321, 421, 42151 and 4216 were all verified by DNA sequencing at Vanderbilt's DNA core facility.

All *E. coli* transformations occurred via commercially available chemically competent cells supplied with the cloning vectors or mutagenesis kits (TOP10 or XL1 blue, respectively) and following manufacturer specifications. All *P. aeruginosa* transformations occurred via electroporation as previously described (Choi *et al.*, 2006).

Colony PCR screen

Sixty-four clinical *P. aeruginosa* isolates were obtained from the Vanderbilt Medical Center Microbiology laboratory in a de-identified fashion. This collection received an exemption from Vanderbilt's Institutional Review Board. Each sample was regrown on MacConkey agar then saved as a frozen

stock for future analysis. The cultures were regrown in 500 μ l of LB broth, pelleted, resuspended in 100 μ l of sterile water and boiled for 10 min. The samples were centrifuged and 1 μ l was used per 25 μ l of PCR reaction. The primers to detect *aguA* (11F and 11R) were designed to amplify a 350 bp region in either PAO1 or PA14. Primers 12F and 12R were used to detect *agu2A*. PCR was performed using the GC Rich PCR system (Roche) and modified annealing temperatures of 60°C for five cycles, reduced by 0.2°C per cycle for the remaining 25 cycles.

Gene expression and protein isolation

Protein expression in *E. coli* occurred using the arabinose inducible promoter in pBAD202 following the manufacturer's protocol. To induce *agu2A*, the culture was grown overnight at 30°C to overcome solubility issues. *Agu2A'* and its mutant derivatives could be induced at either 30°C overnight or 37°C for 4 h in either the pBAD202 or pUCP20 derivatives. Arabinose induction conditions were determined by titration of arabinose at subjective evaluation of protein yield as monitored by Western blotting. The lowest concentration of arabinose for which protein yield appeared to no longer increase was 0.002% for *E. coli* and 0.2% for *P. aeruginosa*.

To harvest total cell protein for analysis or further purification *E. coli* cell pellets were resuspended in 10X Bug Buster (Novagen) that was reconstituted in 50 mM NaCl, 50 mM Na₂PO₄, 0.02% sodium azide with a pH of 8.0 at a ratio of 1.5 ml per 50 ml of overnight culture for *E. coli* or 400 μ l per 10 ml of overnight culture of *P. aeruginosa*. This solution was supplemented with 1/200 v/v Bacterial Protease Inhibitor (Sigma) and 1/1000 v/v Benzonase (Novagen). The cell pellet was gently rocked at RT for 20 min, and centrifuged at 16 000 *g* for 20 min in a microfuge. The supernatant was used directly for enzyme and electrophoretic analysis or loaded onto an imidazole equilibrated nickel resin column. Nickel resin purification of *Agu2A* and *Agu2A'* was performed per the pBAD202 TOPO expression system manufacturer specifications. Protein quantification was performed with the Bradford assay (Bio-Rad) for imidazole containing fractions and the BCA assay (Pierce) for all other samples.

Carbamido detection assay

The assay to detect the products of deimination of the guanidino groups of agmatine and related compounds is derived from the assay for citrulline from Boyd and Rahmatullah (Boyd and Rahmatullah, 1980). Briefly, 100 μ l of sample containing enzyme is mixed with 100 μ l of reaction cocktail containing 10 μ l of 1 M Tris Buffer pH 9, 20 μ l of 500 mM NaCl, 20 μ l of 10 mg ml⁻¹ BSA in water, 10 μ l of 20 mM EDTA, 20 μ l of 50 mM substrate in water, 20 μ l of 10 mg ml⁻¹ Type III Urease (Sigma) in 100 mM phosphate buffer pH 7.0 and 0.2 μ l of 10 mM flavin adenine dinucleotide. The substrates for AgDI, PAD1 and AD1 are agmatine sulfate, benzoyl-arginine ethyl ester, and arginine respectively. To account for background urea, citrulline and other carbamido compounds in the sample formed independent of AgDI activity a 100 μ l sample is incubated with an identical reagent solution replacing the substrate component with water. When crude cell

lysates are analysed urease is added to the reaction to remove the urea component which gives a colorimetric product in the final step. For screening purposes these reactions are incubated in a microfuge tube at 37°C for *Agu2A* and all *P. aeruginosa* extracts and 45°C for *Agu2A'* and its mutants for 1 h and stopped with the addition of 40 μ l of 100% TCA. The reaction is centrifuged at 16 000 *g* for 5 min to remove precipitate and 200 μ l of this mixture is added to 800 μ l of acidified diacetyl monoxime (DAMO). This solution contains a mixture of 5 mg ml⁻¹ DAMO with 0.1 mg ml⁻¹ of thiosemicarbazide mixed one part to two parts of a acid ferric solution which contains 550 ml of water, 250 ml of concentrated sulfuric acid, 200 ml of concentrated phosphoric acid and 250 mg l⁻¹ ferric chloride. The sample and acidified DAMO are incubated for 5 min at 100°C, cooled, centrifuged as before to remove remaining precipitates and transferred in triplicate to a 96-well plate. Carbamido products were measured spectrophotometrically at A_{540nm} using a Bio-Rad 680 plate reader. Citrulline was used to make standard curves in the same buffers used for sample incubation. This assay uses citrulline for the standard curve which has been demonstrated to be less chromogenic than carbamoylputrescine which is not commercially available (Llacer *et al.*, 2007). All specific activities are reported in nanomole of citrulline produced per hour per μ g of protein. The kinetic analysis of purified *Agu2A* and *Agu2A'* was carried out with agmatine concentrations from 30 mM to 100 μ M and time points from 5 min to 2 h. While *Agu2A* was analysed at 37°C, *Agu2A'* was analysed at 25°C to avoid enzymatic degradation which was apparent as early as 5 min at 37°C. Initial velocities were calculated from linear rates usually achieved before 15 min. The K_{cat} calculation for *Agu2A'* was determined using the estimated molecular weight of the enzyme after cleavage of the secretory N-terminal leader. Graph Pad Prism 5 software (Graph Pad software Inc.) was used to perform non-linear regression analysis of the velocity versus substrate graph to determine the K_m and K_{cat}. All chemicals for this assay are from Sigma.

Western blotting

The Nu-Page system by Invitrogen was used for all protein electrophoresis experiments. Manufacturer protocols were used for all steps through transfer to nitrocellulose. The C-terminal 6-His tag antibody from Invitrogen was used as the primary antibody and the anti-mouse IR680 secondary antibody from LiCor was used for detection on the Odyssey digital imaging system (LiCor). The Western blotting technique followed the protocol suggested by the manufacturers of the Odyssey system to minimize background.

Cell fractionation

The technique to separate the various fractions of the *Pseudomonas* cell wall was based on a prior protocol developed for this organism (Snyder *et al.*, 2006). After induction of the bacterial culture as described above, the sample was centrifuged at 12 000 *g* at 4°C for 10 min. The supernatant was removed and proteins were precipitated with a final concentration of 13% TCA at 4°C overnight. The pellet was

air-dried and resuspended in a minimal volume of PBS. The cell pellet was washed in ice cold 20% sucrose at a volume of 50% the original culture volume. The washed cells were weighed and resuspended in 18 ml of 20% ice cold sucrose per 1.5 g of cells. To this, per 1.5 g of cell pellet, the following were added: 9 ml of 2 M Sucrose, 10 ml of 0.1 M Tris (pH 7.8), 1.8 ml of fresh 0.5% (wt/vol) lysozyme and 10 μ l of Benzonase. This solution was gently mixed and placed at 30°C for 30 min. At the 30 min mark 0.8 ml of 150 mM EDTA was added and the sample was returned to 30°C for another 30 min. After this incubation the sample was centrifuged for 20 min at 20 000 g at 4°C. The supernatant was removed and TCA precipitated as described for the culture supernatant. This fraction contains the outer membrane and periplasm. The remaining pellet contains spheroplasts which represents the inner membrane and cytosol. The spheroplasts were washed once in 20% ice cold sucrose, and re-centrifuged as above. The spheroplasts were resuspended in a minimal volume of PBS and immediately boiled for 5 min before either freezing or preparing for protein electrophoresis as described above. Fraction purity was assessed with the nitrocefin and NADH oxidase assays as previously described (Snyder *et al.*, 2006). 15 μ g from each fraction was loaded per lane and analysed with Western blot to the C-terminal His tag as described above.

Promoter analysis

The TSS of the *agu2ABCA'* mRNA was determined using a previously described protocol employing tobacco acid pyrophosphatase (TAP) (Epicentre) processing of mRNA with ligation of a synthetic RNA oligo (Bensing *et al.*, 1996). The mRNA was harvested from stationary phase PA14 grown for 3 additional hours in the presence of 20 mM agmatine using the RNeasy system (Qiagen). After TAP treatment and RNA oligo ligation, the reverse transcription reaction was performed with primer 12R using the Transcriptor High Fidelity cDNA system (Roche). The PCR reaction was performed with primers P1 and 10R and the sequence of the subsequent PCR product was determined at the UMN sequencing facility.

To determine the expression patterns of the *agu2ABCA'* and *aguBA* promoters the plasmids mini-ctx-lacZ, pBW71, pBW72 and pBW73 were transformed into PAO1 and PA14 (WT, *rpoS::Gm*, Δ *lasR* and *aguA::Gm* mutants) by triparental mating using HB101 as described before (Hoang *et al.*, 1998). The Tet^r transconjugates were further subjected to transformation with the pFLP2 plasmid to remove the tetracycline resistance gene and *int* gene as described previously (Hoang *et al.*, 1998). The pFLP2 plasmid was cured by growth on 5% sucrose and the final reporter strains were verified to have insertions into the genomic *attB* site by loss of the 270 bp PCR product of the Pser primers (Becher and Schweizer, 2000; Hoang *et al.*, 2000).

Overnight cultures of each reporter strain were pelleted, resuspended in PBS and repelleted before suspension to an $A_{600\text{nm}}$ of 0.2. 50 μ l of this suspension was used to inoculate 50 ml of LB broth with or without 20 mM agmatine in 125 ml of baffled flasks. These were grown at 37°C in a shaking incubator and 1 ml of aliquots were removed at the respective time points for $A_{600\text{nm}}$ measurement in a UVmini-1240 spectrophotometer (Shimadzu). The detection of β -galactosidase activity

was based on a modified Miller assay and is described with some modification next (Zhang and Bremer, 1995; OpenWetWare, unpublished). 20 μ l of culture from each timepoint was added to 80 μ l of permeabilization solution (100 mM Na_2HPO_4 , 20 mM KCl, 2 mM MgSO_4 , 0.8 mg ml^{-1} CTAB, 0.4 mg ml^{-1} Na deoxycholate, 5.4 μ l ml^{-1} β -mercaptoethanol) before addition of 600 μ l of substrate solution (60 mM Na_2HPO_4 , 40 mM NaH_2PO_4 , 1 mg ml^{-1} ONPG, 2.7 μ l ml^{-1} β -mercaptoethanol). This was allowed to incubate at 37°C until yellow color development and the reaction was stopped with 700 μ l of 1 M Na_2CO_3 and the reaction time recorded. The sample was centrifuged at 16 000 g for 5 min and the $A_{420\text{nm}}$ of the supernatant was measured. Miller units were calculated as $1 \text{ MU} = 1000 \times [A_{420\text{nm}} / (A_{600\text{nm}} \times \text{reaction time (min)} \times \text{culture volume tested in ml})]$. All ABS readings occurred in 1 cm cuvettes and measurement was taken after the measurement reading stabilized. Repeat measurements at either $A_{600\text{nm}}$ or $A_{420\text{nm}}$ typically varied by less than 0.005 ABS units. To analyse the reporter constructs after biofilm growth, the cultures were grown and washed as described below in the biofilm assay and 500 μ l of permeabilization solution was added to each well of the 24-well plates. These wells were sonicated with two 10 s pulses at 50% duty cycle on ice with a VibraCell sonicator (Sonics Materials). 100 μ l of this solution was assayed for β -galactosidase activity as described above. The $A_{420\text{nm}}$ was normalized to the protein content (determined by Pierce Bradford Assay) of the analysed sample as published previously (Sakuragi and Kolter, 2007).

Intracellular agmatine determination

The strains were grown as described in the text and harvested by centrifugation. The cell pellets (~100 mg) were resuspended in PBS and sonicated on ice. The lysate was collected after centrifugation at 20 000 g for 20 min at 4°C and frozen for future use. Internal standard homoagmatine was synthesized from the reaction of cadaverine and cyanamide in boiling 12 N HCl. The crude product mixture was cooled to 0°C, brought to slightly alkaline pH by careful addition of 9 N NaOH, and washed three times with EtOAc. The organic fractions were combined and evaporated to dryness at 50°C under a gentle stream of N_2 gas. The dried extracts were dissolved in $\text{H}_2\text{O}/\text{MeCN}/\text{HCOOH}$ (80:20:0.1) to a final concentration of 2.5 μ M and used without further purification. 100 μ L of thawed lysate was spiked with 10 μ l of homoagmatine, lightly vortexed, allowed to stand at room temperature for 15–20 min and deproteinized with 200 μ l of 2-propanol. Samples were then cooled to –20°C for 45–60 min, and precipitated proteins were removed by centrifugation (18 000 g , 30 min, 4°C). The clear supernatant of each sample was transferred to a membrane dialysis cartridge (3000 MWCO) and filtered at 10°C for 6–8 h (10 000 g). The filtrate was evaporated under a gentle stream of N_2 gas. The residue was reconstituted in 75 μ l of $\text{H}_2\text{O}/\text{CH}_3\text{CN}$ (1:1) containing 20 mM dansyl chloride (Sigma) and 100 mM NaHCO_3 (pH 8.0) and heated to 50°C for 20 min. Following derivatization, samples were diluted with 120 μ l of H_2O and centrifuged to remove particulates (18 000 g , 22°C, 10 min). The clear supernatant was transferred to 200 μ l of silanized autosampler vials equipped with Teflon-lined bonded rubber septa.

A Zorbax SB-C18 *Rapid Resolution HT* column (2.1 mm × 50 mm, 1.8 μm, Agilent Technologies, Palo Alto, CA) equipped with an Acquity UPLC in-line stainless steel filter unit (0.2 μm, Waters) was used for all chromatographic separations. Separations were carried out at room temperature; the autosampler tray temperature was set to 10°C. Mobile phases were made up of 0.5% (v/v) formic acid in (A) H₂O/CH₃CN (95:5) and in (B) H₂O/2-PrOH/CH₃CN (5:10:85). Gradient conditions were as follows: 0–3 min, B = 0%; 3–6 min, B = 0–90%; 6–9 min, B = 90%; 9–10 min, B = 90–0%; 10–15 min, B = 0%. The flow rate was maintained at 350 μl min⁻¹. A software-controlled divert valve was used to transfer eluent from 0 to 4.7 min and from 6 to 15 min of each chromatographic run to waste. The total chromatographic run time was 15 min. The sample injection volume was 20 μl.

Sample analyses were carried out using an Accela UHP quaternary pump and a ThermoPal refrigerated autosampler (Thermo-Fisher Scientific, Waltham, MA). Tandem mass spectrometric detection was performed using a TSQ Quantum Access triple-stage quadrupole mass spectrometer (Thermo-Fisher) equipped with an electrospray ion source and a 100 μm ID deactivated fused silica capillary. The mass spectrometer was operated in positive ion mode. Quantification was based on multiple reaction monitoring (MRM) detection at a collision energy of 30 V (agmatine: *m/z* 364 → 170, homoagmatine: *m/z* 378 → 170).

Data acquisition and quantitative spectral analysis were done using Thermo-Fisher Xcalibur version 2.0.7 and Thermo-Fisher LCQuan version 2.5.6 respectively. Calibration curves were constructed by plotting the peak area ratio (agmatine/homoagmatine) against the concentration of agmatine for a series of six aqueous buffered standards (0.122 μM–243 μM). A weighting factor of 1/C² was applied in the linear least-squares regression analysis to maintain homogeneity of variance across the concentration range. The lower limit of quantification was 122.0 nM, defined as the lowest standard on the calibration curve where %RSD and %RE ≤ 20%.

Biofilm growth and microtiter assay

The biofilm assay used in this study has been described before by O'Toole and Kolter (1998). Briefly overnight cultures grown in LB were pelleted and washed in PBS then diluted to A_{600nm} of 0.2. A 1:100 dilution was made into LB, or LB supplemented with agmatine or Putrescine, and 150 μl was added per well to a Costar 96-well or 24-well polystyrene plate. Samples were tested with eight replicates for 96-well assay or three wells for 24-well assays. For the 96-well crystal violet assay the plates were incubated for 24 h at RT, then washed by repeated dunking in warm tap water, tapped dry and to each well 175 μl of 1% crystal violet was added and placed on a rotating platform for 15 min. The crystal violet was washed out as before staining then 200 μl of DMSO was added to each well and the plate was placed back on the rotating platform for 30 min after which 150 μl of each sample was transferred to a new plate for A_{595nm} measurement.

Statistical analysis

GraphPad InStat software was used to determine statistical significance of the experimental groups. When comparing

two means, *t*-tests were used, and when comparing more than two means, one-way ANOVA was used.

Acknowledgements

We thank Drs H. P. Schweizer, F. Ausubel, G. O'Toole, L. Hoffman and C. Lu for PA plasmids, strains and mutants. We also thank the Vanderbilt Clinical Microbiology lab for saving the clinical isolates used in this study and Dr E. Skaar for critical review of this work, and Dr G. Dunny, C. Johnson and A. Gilbertsen for helpful discussions.

This work was supported by Third and Fourth Year Cystic Fibrosis Foundation Research Fellowship awards to BJW. This work was also supported in part by NIH RO1 HL 61419 and NIH P30 HL 101311-01.

References

- Battaglia, V., Rossi, C.A., Colombatto, S., Grillo, M.A., and Toninello, A. (2007) Different behavior of agmatine in liver mitochondria: inducer of oxidative stress or scavenger of reactive oxygen species? *Biochim Biophys Acta* **1768**: 1147–1153.
- Baumann, S., Sander, A., Gurnon, J.R., Yanai-Balser, G.M., Van Etten, J.L., and Piotrowski, M. (2007) Chlorella viruses contain genes encoding a complete polyamine biosynthetic pathway. *Virology* **360**: 209–217.
- Becher, A., and Schweizer, H.P. (2000) Integration-proficient *Pseudomonas aeruginosa* vectors for isolation of single-copy chromosomal *lacZ* and *lux* gene fusions. *Biotechniques* **29**: 948–950, 952.
- Bendtsen, J.D., Nielsen, H., Widdick, D., Palmer, T., and Brunak, S. (2005) Prediction of twin-arginine signal peptides. *BMC Bioinformatics* **6**: 167.
- Bensing, B.A., Meyer, B.J., and Dunny, G.M. (1996) Sensitive detection of bacterial transcription initiation sites and differentiation from RNA processing sites in the pheromone-induced plasmid transfer system of *Enterococcus faecalis*. *Proc Natl Acad Sci USA* **93**: 7794–7799.
- Boyd, T.R., and Rahmatullah, M. (1980) Optimization of conditions for the colorimetric determination of citrulline, using diacetyl monoxime. *Anal Biochem* **107**: 424–431.
- Campisano, A., Schroeder, C., Schemionek, M., Overhage, J., and Rehm, B.H. (2006) PslD is a secreted protein required for biofilm formation by *Pseudomonas aeruginosa*. *Appl Environ Microbiol* **72**: 3066–3068.
- Choi, K.H., Kumar, A., and Schweizer, H.P. (2006) A 10-min method for preparation of highly electrocompetent *Pseudomonas aeruginosa* cells: application for DNA fragment transfer between chromosomes and plasmid transformation. *J Microbiol Methods* **64**: 391–397.
- D'Argenio, D.A., Wu, M., Hoffman, L.R., Kulasekara, H.D., Deziel, E., Smith, E.E., et al. (2007) Growth phenotypes of *Pseudomonas aeruginosa* lasR mutants adapted to the airways of cystic fibrosis patients. *Mol Microbiol* **64**: 512–533.
- Davies, J.C. (2002) *Pseudomonas aeruginosa* in cystic fibrosis: pathogenesis and persistence. *Paediatr Respir Rev* **3**: 128–134.

- Demady, D.R., Jianmongkol, S., Vuletich, J.L., Bender, A.T., and Osawa, Y. (2001) Agmatine enhances the NADPH oxidase activity of neuronal NO synthase and leads to oxidative inactivation of the enzyme. *Mol Pharmacol* **59**: 24–29.
- Flierl, M.A., Rittirsch, D., Nadeau, B.A., Chen, A.J., Sarma, J.V., Zetoune, F.S., et al. (2007) Phagocyte-derived catecholamines enhance acute inflammatory injury. *Nature* **449**: 721–725.
- Friedman, L., and Kolter, R. (2004) Genes involved in matrix formation in *Pseudomonas aeruginosa* PA14 biofilms. *Mol Microbiol* **51**: 675–690.
- Fukuoka, T., Masuda, N., Takenouchi, T., Sekine, N., Iijima, M., and Ohya, S. (1991) Increase in susceptibility of *Pseudomonas aeruginosa* to carbapenem antibiotics in low-amino-acid media. *Antimicrob Agents Chemother* **35**: 529–532.
- Hoang, T.T., Karkhoff-Schweizer, R.R., Kutchma, A.J., and Schweizer, H.P. (1998) A broad-host-range Flp-FRT recombination system for site-specific excision of chromosomally-located DNA sequences: application for isolation of unmarked *Pseudomonas aeruginosa* mutants. *Gene* **212**: 77–86.
- Hoang, T.T., Kutchma, A.J., Becher, A., and Schweizer, H.P. (2000) Integration-proficient plasmids for *Pseudomonas aeruginosa*: site-specific integration and use for engineering of reporter and expression strains. *Plasmid* **43**: 59–72.
- Kwon, D.H., and Lu, C.D. (2007) Polyamine effects on antibiotic susceptibility in bacteria. *Antimicrob Agents Chemother* **51**: 2070–2077.
- Lee, P.A., Tullman-Ercek, D., and Georgiou, G. (2006) The bacterial twin-arginine translocation pathway. *Annu Rev Microbiol* **60**: 373–395.
- Li, G., Regunathan, S., Barrow, C.J., Eshraghi, J., Cooper, R., and Reis, D.J. (1994) Agmatine: an endogenous clonidine-displacing substance in the brain. *Science* **263**: 966–969.
- Liberati, N.T., Urbach, J.M., Miyata, S., Lee, D.G., Drenkard, E., Wu, G., et al. (2006) An ordered, nonredundant library of *Pseudomonas aeruginosa* strain PA14 transposon insertion mutants. *Proc Natl Acad Sci USA* **103**: 2833–2838.
- Llacer, J.L., Polo, L.M., Tavez, S., Alarcon, B., Hilario, R., and Rubio, V. (2007) The gene cluster for agmatine catabolism of *Enterococcus faecalis*: study of recombinant putrescine transcarbamylase and agmatine deiminase and a snapshot of agmatine deiminase catalyzing its reaction. *J Bacteriol* **189**: 1254–1265.
- Lu, C.D., Itoh, Y., Nakada, Y., and Jiang, Y. (2002) Functional analysis and regulation of the divergent *spuABCDEFGH-spul* operons for polyamine uptake and utilization in *Pseudomonas aeruginosa* PAO1. *J Bacteriol* **184**: 3765–3773.
- Lu, X., Li, L., Wu, R., Feng, X., Li, Z., Yang, H., et al. (2006) Kinetic analysis of *Pseudomonas aeruginosa* arginine deiminase mutants and alternate substrates provides insight into structural determinants of function. *Biochemistry* **45**: 1162–1172.
- Lucas, P.M., Blancato, V.S., Claisse, O., Magni, C., Lolkema, J.S., and Lonvaud-Funel, A. (2007) Agmatine deiminase pathway genes in *Lactobacillus brevis* are linked to the tyrosine decarboxylation operon in a putative acid resistance locus. *Microbiology* **153**: 2221–2230.
- Maeda, T., Wakasawa, T., Shima, Y., Tsuboi, I., Aizawa, S., and Tamai, I. (2006) Role of polyamines derived from arginine in differentiation and proliferation of human blood cells. *Biol Pharm Bull* **29**: 234–239.
- Mah, T.F., Pitts, B., Pellock, B., Walker, G.C., Stewart, P.S., and O'Toole, G.A. (2003) A genetic basis for *Pseudomonas aeruginosa* biofilm antibiotic resistance. *Nature* **426**: 306–310.
- Majumder, S., Wirth, J.J., Bitonti, A.J., McCann, P.P., and Kierszenbaum, F. (1992) Biochemical evidence for the presence of arginine decarboxylase activity in *Trypanosoma cruzi*. *J Parasitol* **78**: 371–374.
- Mercenier, A., Simon, J.P., Haas, D., and Stalon, V. (1980) Catabolism of L-arginine by *Pseudomonas aeruginosa*. *J Gen Microbiol* **116**: 381–389.
- Minic, Z., and Herve, G. (2003) Arginine metabolism in the deep sea tube worm *Riftia pachyptila* and its bacterial endosymbiont. *J Biol Chem* **278**: 40527–40533.
- Nakada, Y., and Itoh, Y. (2003) Identification of the putrescine biosynthetic genes in *Pseudomonas aeruginosa* and characterization of agmatine deiminase and N-carbamoylputrescine amidohydrolase of the arginine decarboxylase pathway. *Microbiology* **149**: 707–714.
- Nakada, Y., Jiang, Y., Nishijyo, T., Itoh, Y., and Lu, C.D. (2001) Molecular characterization and regulation of the *aguBA* operon, responsible for agmatine utilization in *Pseudomonas aeruginosa* PAO1. *J Bacteriol* **183**: 6517–6524.
- Ochsner, U.A., Snyder, A., Vasil, A.I., and Vasil, M.L. (2002) Effects of the twin-arginine translocase on secretion of virulence factors, stress response, and pathogenesis. *Proc Natl Acad Sci USA* **99**: 8312–8317.
- O'Toole, G.A., and Kolter, R. (1998) Initiation of biofilm formation in *Pseudomonas fluorescens* WCS365 proceeds via multiple, convergent signalling pathways: a genetic analysis. *Mol Microbiol* **28**: 449–461.
- Patel, C.N., Wortham, B.W., Lines, J.L., Fetherston, J.D., Perry, R.D., and Oliveira, M.A. (2006) Polyamines are essential for the formation of plague biofilm. *J Bacteriol* **188**: 2355–2363.
- Raasch, W., Regunathan, S., Li, G., and Reis, D.J. (1995) Agmatine, the bacterial amine, is widely distributed in mammalian tissues. *Life Sci* **56**: 2319–2330.
- Reese, M.G. (2001) Application of a time-delay neural network to promoter annotation in the *Drosophila melanogaster* genome. *Comput Chem* **26**: 51–56.
- Regunathan, S., and Piletz, J.E. (2003) Regulation of inducible nitric oxide synthase and agmatine synthesis in macrophages and astrocytes. *Ann N Y Acad Sci* **1009**: 20–29.
- Richards, M.J., Edwards, J.R., Culver, D.H., and Gaynes, R.P. (1999) Nosocomial infections in medical intensive care units in the United States. National Nosocomial Infections Surveillance System. *Crit Care Med* **27**: 887–892.
- Sakuragi, Y., and Kolter, R. (2007) Quorum-sensing regulation of the biofilm matrix genes (*pel*) of *Pseudomonas aeruginosa*. *J Bacteriol* **189**: 5383–5386.
- Salas, M., Rodriguez, R., Lopez, N., Uribe, E., Lopez, V., and Carvajal, N. (2002) Insights into the reaction mechanism of

- Escherichia coli* agmatinase by site-directed mutagenesis and molecular modelling. *Eur J Biochem* **269**: 5522–5526.
- Schuster, M., Hawkins, A.C., Harwood, C.S., and Greenberg, E.P. (2004) The *Pseudomonas aeruginosa* RpoS regulon and its relationship to quorum sensing. *Mol Microbiol* **51**: 973–985.
- Shirai, H., Blundell, T.L., and Mizuguchi, K. (2001) A novel superfamily of enzymes that catalyze the modification of guanidino groups. *Trends Biochem Sci* **26**: 465–468.
- Shirai, H., Mokrab, Y., and Mizuguchi, K. (2006) The guanidino-group modifying enzymes: structural basis for their diversity and commonality. *Proteins* **64**: 1010–1023.
- Snyder, A., Vasil, A.I., Zajdowicz, S.L., Wilson, Z.R., and Vasil, M.L. (2006) Role of the *Pseudomonas aeruginosa* PlcH Tat signal peptide in protein secretion, transcription, and cross-species Tat secretion system compatibility. *J Bacteriol* **188**: 1762–1774.
- Stover, C.K., Pham, X.Q., Erwin, A.L., Mizoguchi, S.D., Warren, P., Hickey, M.J., *et al.* (2000) Complete genome sequence of *Pseudomonas aeruginosa* PA01, an opportunistic pathogen. *Nature* **406**: 959–964.
- Tremblay, J., and Deziel, E. (2008) Improving the reproducibility of *Pseudomonas aeruginosa* swarming motility assays. *J Basic Microbiol* **48**: 509–515.
- Tricot, C., Pierard, A., and Stalon, V. (1990) Comparative studies on the degradation of guanidino and ureido compounds by *Pseudomonas*. *J Gen Microbiol* **136**: 2307–2317.
- Whiteley, M., Bangera, M.G., Bumgarner, R.E., Parsek, M.R., Teitzel, G.M., Lory, S., and Greenberg, E.P. (2001) Gene expression in *Pseudomonas aeruginosa* biofilms. *Nature* **413**: 860–864.
- Wozniak, D.J., Wyckoff, T.J., Starkey, M., Keyser, R., Azadi, P., O'Toole, G.A., and Parsek, M.R. (2003) Alginate is not a significant component of the extracellular polysaccharide matrix of PA14 and PAO1 *Pseudomonas aeruginosa* biofilms. *Proc Natl Acad Sci USA* **100**: 7907–7912.
- Yanagisawa, H. (2001) Agmatine deiminase from maize shoots: purification and properties. *Phytochemistry* **56**: 643–647.
- Zhang, X., and Bremer, H. (1995) Control of the *Escherichia coli* *rrnB* P1 promoter strength by ppGpp. *J Biol Chem* **270**: 11181–11189.

Supporting information

Additional supporting information may be found in the online version of this article.

Please note: Wiley-Blackwell are not responsible for the content or functionality of any supporting materials supplied by the authors. Any queries (other than missing material) should be directed to the corresponding author for the article.